AIP | Applied Physics Letters

Electromagnetic induction by ferrofluid in an oscillating heat pipe

J. G. Monroe, E. S. Vasquez, Z. S. Aspin, K. B. Walters, M. J. Berg, and S. M. Thompson

Citation: Applied Physics Letters **106**, 263901 (2015); doi: 10.1063/1.4923400
View online: http://dx.doi.org/10.1063/1.4923400
View Table of Contents: http://scitation.aip.org/content/aip/journal/apl/106/26?ver=pdfcov
Published by the AIP Publishing

Electromagnetic induction by ferrofluid in an oscillating heat pipe

J. G. Monroe,[1] E. S. Vasquez,[2] Z. S. Aspin,[1] K. B. Walters,[2] M. J. Berg,[3] and S. M. Thompson[1,a)]
[1]*Department of Mechanical Engineering, P.O. Box 9552, Mississippi State University, Mississippi State, Mississippi 39762, USA*
[2]*Dave C. Swalm School of Chemical Engineering, P.O. Box 9595, Mississippi State University, Mississippi State, Mississippi 39762, USA*
[3]*Department of Physics & Astronomy, P.O. Box 5167, Mississippi State University, Mississippi State, Mississippi 39762, USA*

(Received 14 May 2015; accepted 21 June 2015; published online 29 June 2015)

Thermal-to-electrical energy conversion was demonstrated using an oscillating heat pipe (OHP) filled with ferrofluid and equipped with an annular-type solenoid. The OHP was subjected to a 100 °C axial temperature difference allowing the ferrofluid to passively oscillate through the solenoid, thus accomplishing electromagnetic induction. The measured solenoid voltage consisted of aperiodic pulses with dominant frequencies between 2 and 5 Hz and peak-to-peak amplitudes approaching 1 mV. Despite exposure to the thermal and phase change cycling within the OHP, nanoparticle morphologies and magnetic properties of the ferrofluid remained intact. This energy harvesting method allows for combined thermal management and *in-situ* power generation. © *2015 AIP Publishing LLC*. [http://dx.doi.org/10.1063/1.4923400]

An oscillating heat pipe (OHP) is a two-phase heat transfer device that operates passively via an axial temperature difference.[1,2] The device consists of a capillary-sized, serpentine tube, or etched channel that meanders repeatedly between a heat source (evaporator) and heat sink (condenser). The device is evacuated of air (to low vacuum pressure), partially filled with a working fluid and hermetically sealed. Unlike other types of heat pipes, an OHP does not require a wicking structure in order to return liquid from the condenser to the evaporator. Instead, a combative, non-equilibrium vapor pressure field is created in the evaporator due to the non-uniform and asynchronous evaporation/condensation processes. These unstable conditions result in fluid pulsation, typically at frequencies less than 20 Hz,[3–5] between the evaporator and condenser—establishing the cyclic heat pipe mechanism required for high heat transport capability. To initiate and sustain internal fluid motion, a minimum temperature difference (or heat flux) is required to ensure sufficient latent heat transfer for vapor growth.[6–8]

Colloidal suspensions of nanoparticles in a liquid carrier solvent have received significant attention in heat transfer studies over the past several years.[9–11] These "nanofluids" are capable of thermal enhancement,[2,10,11] and have been utilized in OHPs.[2,12–14] Although heat transfer enhancement has been observed with these fluids,[2,13] suspensibility is an ongoing issue, as nanoparticles can settle with time and/or repetitive use as a result of particle aggregation.[13,15] One type of nanofluid is the ferrofluid, which is a suspension of magnetic particles in a liquid solvent.[16] The magnetic nanoparticles used in ferrofluids are typically produced from superparamagnetic magnetite (Fe_3O_4) or ferromagnetic maghemite (Fe_2O_3).[17–19]

Although ferrofluids have been investigated extensively,[20,21] their use in OHPs has generated recent interest.[22,23] For OHPs filled with ferrofluid, an imposed magnetic field can be utilized to control the internal fluid motion and enhance thermal performance, especially when the field is pulsed at an optimal frequency.[22,23] Ferrofluids have also been investigated for their use in energy harvesting and conversion. Bibo *et al*. used a Fe_3O_4 ferrofluid to convert external vibrations (kinetic energy) into electrical energy using two permanent magnets to create a static, bias magnetic field for aligning the dipoles of the Fe_3O_4 particles.[24] Chen *et al*. used a variable speed motor to move a vial of Fe_3O_4 ferrofluid between a pair of Helmholtz coils for creation of a bias field to study the effect of fluid volume and speed on the resulting induction.[25] Recently, Sansom *et al*. demonstrated electrical energy conversion using a Fe_3O_4 ferrofluid within a mechanically pumped system.[26] The ferrofluid was pumped through a 10 mm tube adjacent to, but not passing through, an induction coil and neodymium bias magnet, generating up to 3 mV in the coil.

Thermal energy, in the form of potential (temperature difference) or flux, can be converted to electricity through, for example, the use of the Seebeck effect[27] in thermoelectric materials (TMs) or Stirling engines. Thermoelectric materials (e.g., silicon germanium) have been used in a variety of heat recovery applications including automobile[28] and boiler[29] exhaust streams; with nano-engineering,[30–32] they can achieve efficiencies near ~20%.[33–35] However, since thermoelectric materials typically possess a low thermal conductivity; they are prone to thermomechanical damage and an efficiency that degrades with heat transfer.[36] Stirling engines have found utility in solar harvesting[37] and cogeneration systems[38] with thermal efficiencies in the order of 15%;[37] however, they are often larger than TMs and can require maintenance due to their moving parts.

In the present work, thermoelectricity generation via non-intrusive work extraction from a heat pipe, specifically an OHP, is demonstrated. Unlike other thermoelectric

a)Author to whom correspondence should be addressed. Electronic mail: thompson@me.msstate.edu

generators, the OHP "generator" possesses an ultra-high thermal conductivity that is well-suited for high temperature and/or heat flux applications. Furthermore, this approach demonstrates energy harvesting, via electromagnetic induction, from the passively driven and thermally actuated flow of a ferrofluid—in contrast to the actively pumped (power input required) ferrofluids used in isothermal systems.[26] While the utilization of ferrofluids with an applied magnetic field has been shown to enhance OHP thermal performance, a ferrofluid OHP has not been previously studied as an electromagnetic source. This motivates further investigation into the utilization of thermally driven ferrofluid transport for electromagnetic induction, or "thermofluidic induction."

Ultrapure (type I) water (generated using EMD Millipore Synergy UV) was used for solution preparation and Fe_3O_4 magnetic nanoparticles were synthesized following the method of Massart.[39] In brief, 1 M iron (III) chloride (98%, VWR) and 2 M iron (II) chloride (98%, Sigma Aldrich) solutions were prepared using a 2 M HCl (37%, ACS reagent/Sigma Aldrich) aqueous solution. These iron chloride solutions were combined at a 4:1 volume ratio and mixed for ~5 min. In a separate reactor, 800 ml of a 0.7 M ammonium hydroxide (28–30%, ACS reagent/Sigma Aldrich) solution was stirred at ~600 rpm. The iron solutions were added simultaneously to the NH_4OH solution and the reaction was allowed to proceed for 30 min. A black precipitate was formed and separated using an external neodymium magnetic field. The separated black viscous liquid was water-washed several times until a pH of ~8 was reached and then allowed to dry. The resulting nanoparticles were then re-suspended in 26.5 ml of clean water using sonication (6 h). The total density of the synthesized Fe_3O_4 ferrofluid was ~1.1 g/ml. Note that water was used as the solvent due to its high surface tension; allowing for its capillarity in relatively larger-sized tubes and the opportunity to increase ferrofluid volume for potential harvesting.

To accomplish passive, cyclic thermofluidic induction, the operating principle of a temperature-actuated, ferrofluid OHP (FF-OHP) was exploited. The FF-OHP was constructed by bending copper (phosphorous-deoxidized) capillary tubing (ASTM B280) into a serpentine-arranged cylinder, as shown in Fig. 1. The tube internal diameter ($D_i = 3.25 \pm 0.1$ mm) was selected to ensure capillary action for pure water, i.e., $D_i \lesssim 1.84\sqrt{\gamma/g(\rho_l - \rho_v)}$, where γ is the surface tension, ρ_l is the liquid density, ρ_v is the vapor density, and g is the local gravitational acceleration. As shown in Fig. 1, the cylindrical FF-OHP cylinder has 8 serpentine turns, an overall length of approximately 21.5 cm, and an overall diameter of 6.5 cm. Transparent, temperature-resistant acrylic tubing ($D_i = 3.25 \pm 0.1$ mm) was installed in-line within a section of the FF-OHP to allow for observation of internal fluid oscillation during operation. A coaxial, 1000-turn solenoid 1.6 cm in length was formed using 0.125 mm diameter copper wire, and the solenoid was placed around the acrylic portion of the FF-OHP, as illustrated in Fig. 1.

By attaching an open-section of the OHP (i.e., charging port) to a vacuum pump (Fisher Scientific Maxima M8C) and cold trap assembly, it was evacuated to a vacuum pressure of approximately 3 Pa (± 0.75 Pa). This negative pressure was utilized for filling 70% (±2%) of the OHP's internal volume with ferrofluid. The FF-OHP was then hermetically sealed by pneumatically crimping its charging port. As shown in Fig. 1, the experiment consisted of placing the bottom third of the FF-OHP directly into a "hot" reservoir which was kept at ~100 °C by pumping a synthetic organic heat transfer fluid (Dynalene HT) using a heating circulator (VWR International) located away from the OHP assembly. The top third of the OHP was placed within a custom-made "cold" reservoir kept at ~0 °C (ice bath).

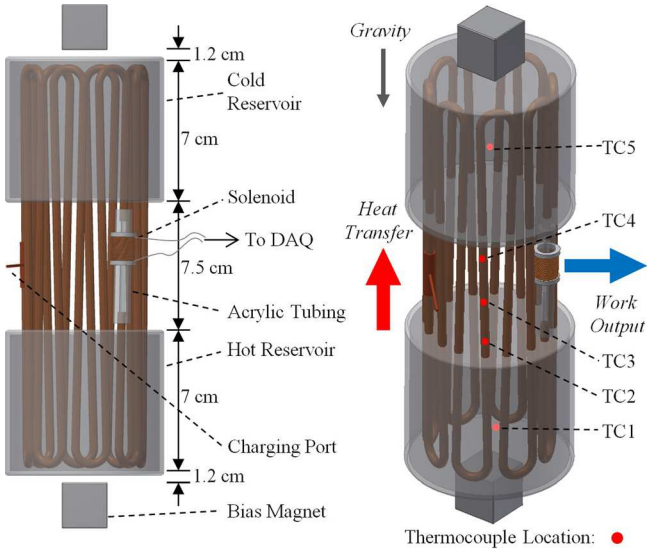

FIG. 1. Front view of FF-OHP with dimensions and harvesting setup (left) and isometric view with marked thermocouple locations (right).

As shown in Fig. 1, two neodymium "bias" magnets (16.4 cm^3 cubes, Grade N40, 334.3 ± 0.05% N optimal pull strength) were positioned at opposite ends of the OHP for creating a quasi-uniform magnetic field with ellipsoidal-shape. This field partially aligns the magnetic domains of the iron oxide nanoparticles prior to harvesting—allowing for generation of a transient magnetic flux through the external solenoid as the ferrofluid moves, thus inducing an electric potential across the solenoid terminals.

The experiment was designed to measure the temperature and voltage response of the FF-OHP as it was introduced to an axial temperature difference. As shown in Fig. 1, the setup consisted of the FF-OHP (oriented parallel with gravity), hot and cold reservoirs, a solenoid, bias magnets, and a data acquisition system (National Instruments cDAQ-9178 chassis with NI 9213/temperature and NI 9205/voltage modules) that relayed temperature and voltage measurements to a computer equipped with LabVIEW SignalExpress 2012.

Figure 1 shows the location of five type-T thermocouples (Omega, ± 1 °C) that measured temperatures along the OHP length; three thermocouples were placed along the surface of a tube near the harvesting section (TC2-TC4) and two were placed in the hot and cold reservoirs (TC1 and TC5, respectively). The portion of the FF-OHP between the reservoirs was wrapped in fiberglass insulation except for the harvesting tube, which was uncovered to allow for visual inspection of the internal flow. Temperature measurements were collected at a rate of 120 Hz. The experiment lasted approximately 5 min, ceasing once the imposed thermal gradient across the OHP became insufficient to drive fluid motion due to sensible heating of the cold reservoir.

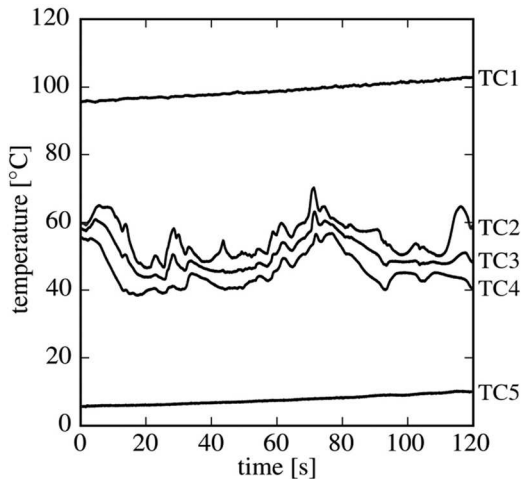

FIG. 2. Measured temperatures for the hot reservoir (TC1), FF-OHP tube section (TC2-TC4), and cold reservoir (TC5).

To prevent high frequency electronic noise from interfering with voltage measurements, the solenoid voltage signal was routed through a passive, 40 Hz low-pass filter. To eliminate aliasing issues, voltage data were collected at 800 Hz. Finally, a 40th order, 45 Hz Butterworth low-pass filter was employed (via LabVIEW) to remove any residual 60 Hz noise from local electrical power sources. Significant efforts were made to minimize electromagnetic interference from surrounding instruments and sources.

The FF-OHP was found to start operating after the thermal gradient was applied, as evidenced by temperatures TC2–TC4 quickly starting to oscillate with respect to time (Fig. 2). The temperature oscillations exhibited multi-frequency characteristics with peak-to-peak amplitudes as high as ~30 °C. The ferrofluid was observed to pulsate as a vapor/liquid mixture (predominantly liquid) along the acrylic tube section with near-random frequency. The appearance and behavior of the ferrofluid did not visibly change during the test duration, indicating no gross aggregation or settling due to repeated thermal cycling and phase change. The heat transport capability of the FF-OHP resulted in TC5 (cold reservoir) rising in temperature (~5 °C during the 2 min data collection time).

During FF-OHP operation, the coaxial solenoid was observed to produce a time-varying voltage with peak-to-peak amplitude of ~0.8 mV, as shown in Fig. 3(a). The voltage signal was aperiodic and consisted of low-frequency spikes attributed to the pseudo-random fluid motion within the FF-OHP. A shorter time window of the signal is shown in Fig. 3(a) (inset) and illustrates the low amplitude behavior. A time-averaged frequency spectrum of the root mean square (RMS) voltage was generated using short-time Fourier transforms (STFTs)[4] and is shown in Fig. 3(b). The spectrum demonstrates that the maximum voltage generation occurs at lower frequencies, i.e., 2–5 Hz, and the amplitude decreases as frequency increases. Peak generated power was estimated to be in the order of ~1 nW. Note that the temperature and voltage signals (Figs. 2 and 3) are not directly in-phase due to each being recorded from different OHP tubes.

The thermal efficiency of the investigated system is inevitably low due to the very high heat transfer ability of the FF-OHP. Its direct comparison to other, more proven, conversion methods, such as TMs and Stirling engines, would prejudice its dual functionality as both a thermal management device and power generator. The experimental results aim to demonstrate and confirm non-intrusive/passive work extraction from a heat pipe, specifically via thermofluidic induction. The FF-OHP and harvesting method can be further optimized for the task of thermal-to-electrical conversion by employing: more solenoids, flow that is less-dependent on temperature difference, and alternate nanoparticle/fluid combinations.

To examine the impact of OHP operation on the ferrofluid, the morphological and magnetic characteristics of the ferrofluid were examined using transmission electron microscopy (TEM) and atomic/magnetic force microscopy (AFM/MFM). The Fe_3O_4 ferrofluid solution was diluted (10 μl in 1.5 ml of ultrapure water), a drop deposited on a 300 mesh copper grid/glass slide, and the sample was allowed to dry for approximately 12 hours. TEM images were collected using a JEOL JEM-2100 operated at 200 kV. AFM and MFM images were collected using a Dimension Icon instrument (Bruker) and Si cantilever with a Co-Cr coated tip (MESP, Bruker) under ambient conditions. For the MFM measurements, the Si cantilever was magnetized by placing it on an external magnet for 10 s, and a 100 nm lift height was utilized when collecting data.

The morphological and magnetic characteristics of the ferrofluid are shown in Fig. 4. Spherical Fe_3O_4 primary particles (7–10 nm) were observed with TEM, as shown in Fig.

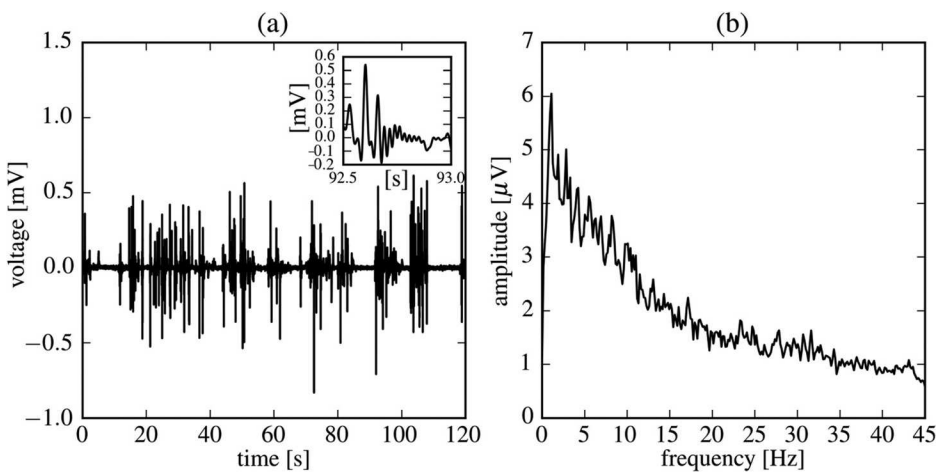

FIG. 3. Measured FF-OHP solenoid voltage: (a) time-series and (b) signal spectrum.

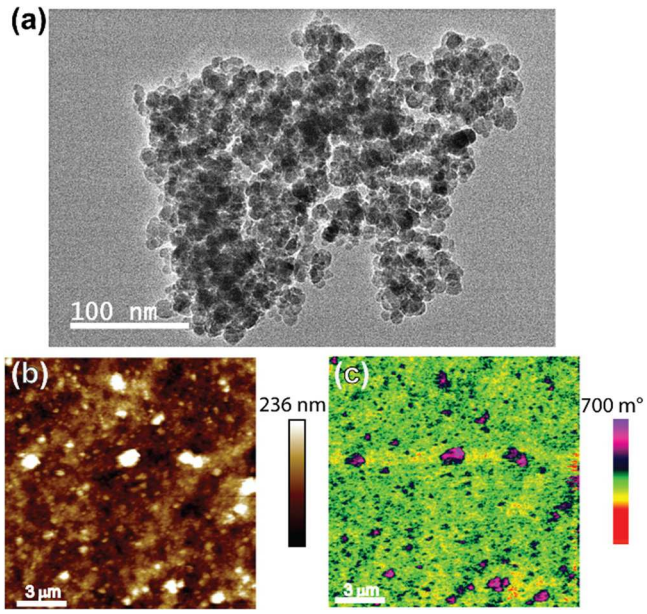

FIG. 4. Morphological and magnetic ferrofluid characterization: (a) TEM, (b) AFM topography, and (c) MFM lift-phase signal demonstrating the magnetic response of the ferrofluid nanoparticles and aggregates.

4(a). Primary particle size was confirmed by analyzing particle heights using AFM topography data provided in Fig. 4(b). The larger-scale clusters/aggregates (up to 1 μm) observed with TEM and AFM are attributed to the drying of the nanoparticle solution prior to imaging. The ferrofluid nanoparticles demonstrated spherical morphology of the primary particles before and after OHP servicing. With MFM, nanoscale magnetic domain data of the Fe_3O_4 nanoparticles were collected using a phase-shift signal with a magnetized AFM tip.[40] Using a lift height of 100 nm, a strong magnetic signal was measured for the dried ferrofluid sample, as shown in Fig. 4(c). This strong magnetic response was measured even after the ferrofluid was subjected to multiple phase change/heating cycles within the OHP.

An OHP has been experimentally demonstrated as a means to accomplish thermofluidic induction. When partially filled with ferrofluid and positioned between a sufficient temperature gradient and magnetic field, the OHP can produce electromagnetic induction in an external solenoid. This is due to alignment of the particles' magnetic moments and the thermally actuated, oscillatory fluid motion within the OHP structure. The investigated ferrofluid OHP (i.e., FF-OHP) was shown to produce a time-varying voltage across the solenoid, with low-frequency (1–5 Hz) spikes and peak-to-peak amplitudes approaching 1 mV. Future work should focus on tailoring the OHP, which has been used primarily for thermal management, for the dedicated role of power generation.

This work was funded by the National Science Foundation (CBET-1403872, CBET-0923474, IIA-1430364, EPS-0903787, and DBI-1126743). We acknowledge TEM/AFM assistance provided by Dr. I-Wei Chu at the Institute for Imaging and Technical Technologies (I2AT) at Mississippi State University.

[1]H. Akachi, U.S. patent 4,921,041 (May 1, 1990).
[2]H. B. Ma, C. Wilson, B. Borgmeyer, K. Park, Q. Yu, S. U. S. Choi, and M. Tirumala, Appl. Phys. Lett. **88**, 143116 (2006).
[3]O. Suzuki, Trans. Jpn. Soc. Mech. Eng., B **69**, 430 (2003).
[4]J. D. Fairley, S. M. Thompson, and D. Anderson, Int. J. Therm. Sci. **91**, 113 (2015).
[5]H. B. Ma, B. Borgmeyer, P. Cheng, and Y. Zhang, J. Heat Transfer **130**, 081501 (2008).
[6]Y. Zhang and A. Faghri, Heat Transfer Eng. **29**, 20 (2008).
[7]J. L. Xu and X. M. Zhang, Heat Mass Transfer **41**, 685 (2005).
[8]W. Qu and H. B. Ma, Int. J. Heat Mass Transfer **50**, 2309 (2007).
[9]S. U. S. Choi, Z. G. Zhang, W. Yu, F. E. Lockwood, and E. A. Grulke, Appl. Phys. Lett. **79**, 2252 (2001).
[10]D. Y. Tzou, Int. J. Heat Mass Transfer **51**, 2967 (2008).
[11]S. K. Das, S. U. S. Choi, and H. E. Patel, Heat Transfer Eng. **27**, 3 (2006).
[12]Y. H. Lin, S. W. Kang, and H. L. Chen, Appl. Therm. Eng. **28**, 1312 (2008).
[13]P. Cheng, S. Thompson, J. Boswell, and H. B. Ma, J. Electron. Packag. **132**, 041009 (2010).
[14]Y. Ji, H. Ma, F. Su, and G. Wang, Exp. Therm. Fluid Sci. **35**, 724 (2011).
[15]L. Fedele, L. Colla, S. Bobbo, S. Barison, and F. Agresti, Nanoscale Res. Lett. **6**, 300 (2011).
[16]R. E. E. Rosensweig, J. Magn. Magn. Mater. **252**, 370 (2002).
[17]N. Pamme, Lab Chip **6**, 24 (2006).
[18]X. Y. Yang, L. Chen, B. Han, X. L. Yang, and H. Duan, Polymer (Guildf). **51**, 2533 (2010).
[19]A. K. Bajpai and R. Gupta, Polym. Compos. **31**, 245 (2010).
[20]S. Odenbach, J. Phys. Condens. Matter **16**, R1135 (2004).
[21]L. Sprenger, A. Lange, and S. Odenbach, Phys. Fluids **26**, 022001 (2014).
[22]M. Mohammadi, M. Mohammadi, A. R. Ghahremani, M. B. Shafii, and N. Mohammadi, Heat Transfer Eng. **35**, 25 (2014).
[23]N. Zhao, D. Zhao, and H. Ma, J. Therm. Sci. Eng. Appl. **5**, 011005 (2013).
[24]A. Bibo, R. Masana, A. King, G. Li, and M. F. Daqaq, Phys. Lett. A **376**, 2163 (2012).
[25]C.-Y. Chen, S.-Y. Wang, C.-M. Wu, C.-H. Lin, and K.-A. Huang, Magnetohydrodynamics **48**, 567 (2012).
[26]C. L. Sansom, P. Jones, R. A. Dorey, C. Beck, A. Stanhope-Bosumpim, and J. Peterson, J. Magn. Magn. Mater. **335**, 159 (2013).
[27]T. J. Seebeck, Abh. Akad. Wiss. Berlin **1820–1821**, 289–346 (1822).
[28]C.-T. Hsu, G.-Y. Huang, H.-S. Chu, B. Yu, and D.-J. Yao, Appl. Energy **88**, 1291 (2011).
[29]N. R. Kristiansen, G. J. Snyder, H. K. Nielsen, and L. Rosendahl, J. Electron. Mater. **41**, 1024 (2012).
[30]B. Gahtori, S. Bathula, K. Tyagi, M. Jayasimhadri, A. K. Srivastava, S. Singh, R. C. Budhani, and A. Dhara, Nano Energy **13**, 36 (2015).
[31]C. J. Vineis, A. Shakouri, A. Majumdar, and M. G. Kanatzidis, Adv. Mater. **22**, 3970 (2010).
[32]M. S. Dresselhaus, G. Chen, M. Y. Tang, R. G. Yang, H. Lee, D. Z. Wang, Z. F. Ren, J.-P. Fleurial, and P. Gogna, Adv. Mater. **19**, 1043 (2007).
[33]J. Sootsman, D. Y. Chung, and M. G. Kanatzidis, Angew. Chem. Int. Ed. **48**, 8616 (2009).
[34]L. E. Bell, Science **321**, 1457 (2008).
[35]D. M. Rowe, *Thermoelectrics Handbook: Macro to Nano* (CRC Press, 2005).
[36]Z. Tian, S. Lee, and G. Chen, ASME J. Heat Transfer **135**, 061605 (2013).
[37]A. Kribus, J. Sol. Energy Eng. **124**, 189 (2002).
[38]T. Li, D. Tang, Z. Li, J. Du, T. Zhou, and Y. Jia, Appl. Therm. Eng. **33–34**, 119 (2012).
[39]R. Massart, IEEE Trans. Magn. **17**, 1247 (1981).
[40]H. Li, X. Qi, J. Wu, Z. Zeng, J. Wei, and H. Zhang, ACS Nano **7**, 2842 (2013).